New Phytologist

Research

Arabidopsis ZED1-related kinases mediate the temperature-sensitive intersection of immune response and growth homeostasis

Zhicai Wang[1,2]*, Dayong Cui[1,3]*, Jing Liu[1]*, Jingbo Zhao[1], Cheng Liu[1,2], Wei Xin[1], Yuan Li[4], Na Liu[5], Dongtao Ren[4], Dingzhong Tang[5] and Yuxin Hu[1,6]

[1]Key Laboratory of Plant Molecular Physiology, CAS Center for Excellence in Molecular Plant Sciences, Institute of Botany, Chinese Academy of Sciences, Beijing 100093, China; [2]University of Chinese Academy of Sciences, Beijing 100049, China; [3]School of Life Sciences, Qilu Normal University, Jinan 250200, China; [4]State Key Laboratory of Plant Physiology and Biochemistry, College of Biological Sciences, China Agriculture University, Beijing 100193, China; [5]State Key Laboratory of Plant Cell and Chromosome Engineering, Institute of Genetics and Developmental Biology, Chinese Academy of Sciences, Beijing 100101, China; [6]National Center for Plant Gene Research, Beijing 100093, China

Author for correspondence:
Yuxin Hu
Tel: 861062836650
Email: huyuxin@ibcas.ac.cn

Received: *29 December 2016*
Accepted: *23 March 2017*

New Phytologist (2017)
doi: 10.1111/nph.14585

Key words: ambient temperature, *Arabidopsis*, growth homeostasis, HOPZ-ETI-DEFICIENT 1 (ZED1)-related kinase, immune response, SUPPRESSOR OF NPR1-1 CONSTITUTIVE 1 (SNC1).

Summary

- Activation of the immune response in plants antagonizes growth and development in the absence of pathogens, and such an autoimmune phenotype is often suppressed by the elevation of ambient temperature. However, molecular regulation of the ambient temperature-sensitive intersection of immune response and growth is largely elusive.
- A genetic screen identified an *Arabidopsis* mutant, *zed1-D*, by its high temperature-dependent growth retardation. A combination of molecular, cytological and genetic approaches was used to investigate the molecular basis behind the temperature-sensitive growth and immune response in *zed1-D*.
- A dominant mutation in HOPZ-ETI-DEFICIENT 1 (ZED1) is responsible for a high temperature-dependent autoimmunity and growth retardation in *zed1-D*. The autoimmune phenotype in *zed1-D* is dependent on the HOPZ-ACTIVATED RESISTANCE 1 (ZAR1). ZED1 and some ZED1-related kinases (ZRKs) are induced by elevated temperature and function cooperatively to suppress the immune response by modulating the transcription of *SUPPRESSOR OF NPR1-1 CONSTITUTIVE 1* (*SNC1*) in the absence of pathogens.
- Our data reveal a previously unidentified role of ZRKs in the ambient temperature-sensitive immune response in the absence of pathogens, and thus reveals a possible molecular mechanism underlying the temperature-mediated intersection of immune response and growth in plants.

Introduction

Sessile plants have to integrate a wide variety of environmental cues, such as light, temperature, and other biotic and abiotic signals, into their developmental programmes to prioritize morphogenesis for successful reproduction. Increasing evidence has suggested that plant growth is intricately intertwined with the immune response in the absence of pathogens, and such antagonistic interaction appears to be greatly influenced by ambient temperature (Mittler *et al.*, 1995; Gomez-Gomez *et al.*, 1999; Molina *et al.*, 1999; Huot *et al.*, 2014). For example, a large number of identified *Arabidopsis* mutants with autoimmune responses, including *suppressor of npr1-1 constitutive 1* (*snc1*), *bonzai1-1* (*bon1-1*), *chilling-sensitive 2* (*chs2*), *chs3* and *suppressor of salicylic acid insensitivity of npr1-5* (*ssi4*), exhibit growth retardation at comparatively low temperature conditions, yet such autoimmune phenotypes are often suppressed by the elevation of ambient temperature (Zhang *et al.*, 2003; Yang & Hua, 2004; Zhou *et al.*, 2008; Huang *et al.*, 2010; Yang *et al.*, 2010). Likewise, the *Arabidopsis* F_1 incompatible hybrids or their progenies among different accessions also display an inappropriate activation of defense responses and an inhibition of development at 14–16°C, and this phenotype is alleviated or abolished at 22–23°C (Bomblies *et al.*, 2007; Alcazar *et al.*, 2009), demonstrating that ambient temperature plays a critical role in balancing plant growth homeostasis by antagonizing the immune response under normal growth conditions.

Plants have evolved a large number of resistance (R) proteins, which contain a nucleotide-binding site (NB), C-terminal leucine-rich repeats (LRR), and either a Toll/Interleukin-1-receptor-like (TIR) or a coiled-coil (CC) domain at the N-terminus, to detect the specific pathogen effector and trigger defense response (Jones & Dangl, 2006). Although the R proteins are essential for the pathogenic effector-triggered immunity

*These authors contributed equally to this work.

(ETI), the activation of their activity in the absence of pathogens is detrimental to normal growth and development, and thus needs to be tightly controlled (McDowell & Simon, 2006). The *Arabidopsis* SNC1 belongs to a TIR-NB-LRR type of R proteins that is proposed to activate the systemic acquired resistance (SAR) (Zhang *et al.*, 2003; Johnson *et al.*, 2012). The gain-of-function mutant of *SNC1*, *snc1-1* or *bal/snc1-2*, exhibits a temperature-sensitive dwarfism with autoimmunity (Stokes *et al.*, 2002; Zhang *et al.*, 2003), whereas loss-of-function of *SNC1* in the *snc1-11* could partially or completely suppress the phenotypes of some low-temperature-sensitive autoimmune mutants, including *bon1*, *bap1* (*bon association protein 1*), *bir1* (*bak1-interating receptor-like kinase 1*), *cpr1* (*constitutive expressor of PR gene 1*) and *mkp1* (*map kinase phosphatase 1*) (Yang & Hua, 2004; Yang *et al.*, 2006; Bartels *et al.*, 2009; Cheng *et al.*, 2011; Wang *et al.*, 2011b). Moreover, recent studies also suggest that the high temperature-induced reduction of nucleus-accumulated TIR type NB-LRR proteins, including SNC1, might be responsible for the dampened ETI under high temperature conditions (Zhu *et al.*, 2010; Mang *et al.*, 2012), suggesting that the tight control of SNC1 or possibly other R proteins might be a regulatory mechanism underlying the temperature-sensitive intersection of immunity and growth. However, the molecular link of ambient temperature and these R proteins has remained elusive.

The *Arabidopsis* ZED1 and ZED1-related kinases (ZRKs) belong to a receptor-like cytoplasmic kinase (RLCK) XII-2 subfamily (Lehti-Shiu & Shiu, 2012). ZED1 is shown to interact with ZAR1 and is required for the recognition of the *Pseudomonas syringae* secreted type III effector HopZ1a (Lewis *et al.*, 2013). HopZ1a directly acetylates on threonine 125 and 177 of ZED1 to trigger a HopZ1a-specific ETI response (Lewis *et al.*, 2013). Recent study also reveals that another ZRK member, ZRK1/RKS1 (RESISTANCE RELATED KINASE 1), is required for the *Xanthomonas campestris* effector AvrAC/XopAC-triggered ETI (Wang *et al.*, 2015). Interestingly, the recognition of AvrAC also requires the preformed complex of ZRK1-ZAR1 (Wang *et al.*, 2015), implying that ZAR1 might be involved in multiple ZRK-ZAR1 complexes for effector-induced immune responses. The RLCK XII-2 gene subfamily contains 13 *ZRK*s that are clustered on the chromosome 1 and 3 (Lewis *et al.*, 2013). However, ZED1 and ZRK1 are shown to function as pseudokinases, whereas ZRK10 seems to be a functional kinase (Lewis *et al.*, 2013; Wang *et al.*, 2015), implying that the ZRK family members may function differentially or execute their biological functions in different ways.

Here, we report that *Arabidopsis* ZED1 and ZRKs are involved in regulation of the ambient temperature-sensitive intersection of immune response and growth in the absence of pathogens. We show that a dominant mutation in *ZED1* confers plants with high temperature-induced autoimmunity and growth retardation in a ZAR1-dependent manner. We further demonstrate that *ZED1* and some *ZRK* genes are induced by high temperatures and cooperatively inhibit the immune response by suppressing the transcription of *SNC1* in the absence of pathogens. These results thus define an unidentified role of ZRKs in balancing growth and the immune response in response to ambient temperatures in plants.

Materials and Methods

Plant materials and growth conditions

The *Arabidopsis thaliana* (L.) Heynh. accessions Columbia-0 (Col-0) and Landsberg *erecta* (L*er*) were used in this study. The *zed1-6* (SALK_018065), *zrk12-1* (SALK_113950) and *zar1-3* (Salk_033548) mutants were obtained from the Arabidopsis Biological Resource Center (ABRC). The *snc1-2*, *snc1-11*, and transgenic *nahG* plants were described previously (Bowling *et al.*, 1994; Yang & Hua, 2004). All plants were grown in a controlled culture room or growth chamber with an illumination intensity of 80–90 $\mu mol\ m^{-2}\ s^{-1}$ and a 16 h : 8 h, light : dark photoperiod, as described previously (Jing *et al.*, 2009).

Plasmid construction

In order to generate the *p35S::ZED1*, *p35S::ZED1-D*, *p35S::ZRK* and *p35S::ZAR1* constructs, the coding sequences of *ZED1*, *ZED1-D*, *ZRK*s or *ZAR1* were ligated into the pEasy-Blunt vector (TransGen, Beijing, China), and cloned into the pVIP96 or pVIP96myc plasmid (Hu *et al.*, 2003). A DNA fragment containing the 2-kb *ZED1* promoter and *ZED1* coding region was fused with the β-*glucuronidase* (*GUS*) gene and cloned into the pBI101 plasmid, and the 3′UTR region of *ZED1* was then ligated into the end of the *GUS* gene to form the *pZED1::ZED1-GUS* construct. For generation of the *pZED1::ZED1-GFP* and *pZED1:: ZED1-D-GFP* constructs, the *ZED1* promoter and their coding sequences were fused with *GFP* and cloned into the pCAMBIA1300 vector. To generate *p35S::ZED1-GFP*, *p35S::ZED1-D-GFP*, *p35S::ZED1*^{T177A}*-GFP* and *p35S::ZED1-D*^{T177A}*-GFP* constructs, the coding sequences of *ZED1*, *ZED1-D* or mutated *ZED1* or *ZED1-D* were fused with *GFP* and cloned into the pH7WGF2 vector. All of the primers used for plasmid construction are listed in Supporting Information Table S1.

Cytological analyses and microscopy

The inflorescence stems, leaf lamina and petioles of *zed1-D* and wild-type (WT) plants were excised and cleared with chloral hydrate, and then visualized under a microscope. The specimens of elongated inflorescence stems were doubly fixed in formaldehyde-acetic acid-alcohol (FAA) and osmium tetroxide, and then dehydrated in an ascending grade series of alcohol solutions, cleared in propylene epoxide, and embedded in EPON 812 epoxy resin. The semi-thin sections (1 μm) were stained with 0.1% toluidine blue and photographed under a microscope. The cell length and width were measured with ImageJ software (http://rsbweb.nih.gov/ij/). The shoot apices of WT and transgenic *p35S::ZED1-D* plants were fixed in fresh FAA solution and then scanned with a scanning electron microscope (SEM). For lignin staining, hand-made cross-sections of inflorescence stems were incubated in phloroglucin solution (saturated in 20% HCl) for 2 min, rinsed in de-ionized water, and then photographed under a microscope. To determine the subcellular localization of ZED1 and ZED1-D, 1-wk-old transgenic plants harboring the

corresponding *GFP*-fused construct were used for visualizing green fluorescent protein (GFP) signals. The GFP fluorescence in the specific cells was excited at 488 nm and monitored at 505–550 nm with a pinhole setting at 1.5 au under a confocal microscope (Leica TCS SP5; Leica, Mannheim, Germany).

Cloning of *ZED1* and gene expression analyses

A map-based cloning approach, based on simple sequence length polymorphism (SSLP) and cleaved amplified polymorphic sequence (CAPS) markers, was carried out to identify the candidate mutation in *zed1-D* in an F_2 population of *zed1-D* crossed with L*er*. The genes within a finely mapped genomic region in *zed1-D* were sequenced.

The total RNA was isolated using a guanidine thiocyanate extraction buffer, as described previously (Hu *et al.*, 2000). The reverse transcription PCR (RT-PCR), quantitative real-time reverse transcription PCR (qRT-PCR) and the histochemical GUS assay were carried out according to the previously described protocols (Cui *et al.*, 2013). For RNA *in situ* hybridization, a cDNA region of *ZED1* was transcribed *in vitro* to generate sense and antisense probes using a Digoxigenin RNA labeling kit (Roche, Switzerland). The inflorescence was fixed and embedded in paraffin and then sectioned to 10 μm thickness. The sections were pretreated, hybridized, washed and analyzed as described previously (Fobert *et al.*, 1994).

RNA-Seq analysis

The WT and *zed1-D* plants were grown at 18°C until the primary inflorescence stem bolted to 0.5–1.0 cm, and then transferred into 28°C. Inflorescences with juvenile leaves were harvested at 0, 3, 12 and 48 h for total RNA isolation. The mRNA was purified with magnetic (dT) beads, and fragmented to a size of *c.* 200 bp. The resulting fragments were synthesized as double-stranded cDNA molecules, and the ends were modified by adding an adenine to the 3′ terminus. Sequencing was performed with two biological replicates, using the Illumina HiSeq™ 2000 platform at the Beijing Genomics Institute (BGI, Shenzhen, China). The differentially expressed genes were subjected to GO and KEGG Ontology (KO) enrichment analysis based on hypergeometric tests. The RNA-Seq data has been deposited in the GEO database under the accession number GSE95665.

Immune staining assays

For Trypan Blue (TB) staining, the detached rosette leaves were placed into the centrifuge tubes containing TB staining solution. The samples were heated in a water bath for 5 min, cleared overnight in chloral hydrated solution, and observed under a microscope (van Wees, 2008). For the 3,3′-diaminozenzidine (DAB) staining, the aerial organs of 4-wk-old plants grown at either 18 or 25°C were collected and vacuumed in DAB solution for 5 min, and then shaken for 4 h at 100 rpm, and de-stained in 100% ethanol for 3 h (Clarke, 2009).

Protein extraction and immunoblot analysis

In order to examine the cellular accumulation of ZED and ZED1-D, transgenic seedlings harboring the corresponding *GFP*-fused construct were harvested, ground in liquid nitrogen and suspended in lysis buffer (20 mM Tris-HCl, pH 7.5, 20 mM KCl, 2 mM EDTA, 2.5 mM $MgCl_2$, 25% glycerol, protease inhibitor cocktail) on ice. The suspension was filtered through double layers of miracloth and then centrifuged at 1500 ***g*** for 10 min. The supernatant was then centrifuged at 10 000 ***g*** for 10 min at 4°C, and thus the cytoplasmic fraction was obtained. The nuclear fraction was isolated from the pellet as described previously (Wang *et al.*, 2011a). The cytoplasmic and nuclear protein extracts were loaded on a 10% sodium dodecyl sulfate–polyacrylamide gel (SDS-PAGE) for protein separation, and the proteins were immunobloted by anti-GFP antibody (MBL, Nagoya, Japan), as described previously (Liu *et al.*, 2010). The Histone H3 and β-ACTIN were used as internal controls for the nuclear and cytosolic proteins, respectively.

Co-immunoprecipitation (CoIP) assay

In order to validate interactions between ZED1, ZED1-D and ZAR1 *in planta*, total protein samples were extracted with a cell lysis buffer (50 mM Tris-HCl, pH 7.5, 150 mM NaCl, 10% glycerol, 10 mM DTT, 10 mM EDTA, 1 mM NaF, 1 mM $Na_2MoO_4{\cdot}2H_2O$, 1% polyvinylpyrrolidone and protease inhibitor cocktail) from *Arabidopsis* transgenic plants. The extracts were incubated for 4 h at 4°C with 50 μl of anti-GFP antibody conjugated in micro beads (MBL), and the beads were then washed at least four times (Roux *et al.*, 2011). The proteins bound to the beads were fractionated in SDS-PAGE gel and probed with anti-GFP or anti-MYC antibody (MBL).

Kinase activity assay

In order to detect kinase activity, *ZED1* and *ZED1-D* were cloned into the pET-32a (+) vector. Recombinant proteins expressed in *Escherichia coli* BL21 cells were purified via a Ni Sepharose 6 Fast Flow immobilized metal ion affinity chromatography (IMAC) (GE Healthcare, Stockholm, Sweden). The *in vitro* kinase assay was performed by incubating 2 μg of purified recombinant proteins in kinase assay buffer (30 μl) containing 25 mM Tris-HCl, pH 7.5, 10 mM cofactor Mn^{2+}, 1 μCi [γ-^{32}P] ATP and 5 μg myelin basic protein (MBP) at 30°C for 10 min, and then 10 μl of 4× SDS loading buffer was added to stop the reaction (Xu *et al.*, 2008). The kinase domain of BRASSINOSTEROID INSENSITIVE 1 (BRI1) was used as a positive control.

Results

zed1-D exhibits a high temperature-dependent growth retardation

In order to identify the key factor controlling plant organogenesis, we performed a genetic screen in *Arabidopsis* to isolate the

mutants with altered morphogenesis of aerial organs (Hu *et al.*, 2010; Cui *et al.*, 2013). A dwarf mutant was identified by its severely shortened inflorescence stem with clustered siliques (Figs 1a, S1a). This mutant was initially designated as *clustered silique* (*cls*) and subsequently as *zed1-D* (see later). Besides the strikingly shortened inflorescence stems, the *zed1-D* plants also displayed the pleiotropic phenotype in their aerial organs, including crinkled lamina, shortened petiole, reduced pedicel length and silique numbers, and increased branches (Fig. 1a; Table S2). Detailed cytological examination revealed that the cell elongation and/or expansion in *zed1-D* inflorescence stem, petioles and lamina were substantially inhibited, and that the differentiation of trichomes and stomata was disturbed in epidermis of *zed1-D* inflorescence stems (Figs 1b,c, S1b–d). Moreover, when compared with those of WT, the *zed1-D* inflorescence stem had disorganized interfascicular fibers and fewer pith tissues (Fig. 1d), and more abundant lignin deposition was observed in the *zed1-D* vasculatures (Fig. S1e). These observations indicate that the mutation in *zed1-D* has pleiotropic effects on aerial organ development.

Interestingly, we observed that the pleiotropic phenotype of *zed1-D* was highly dependent on ambient temperature. When grown at or below 22°C, the *zed1-D* plants were found to be indistinguishable from WT plants, whereas the typical dwarfism was only observed when *zed1-D* plants were grown at 24°C or above temperature condition (Fig. 1e). When grown at 23°C, the *zed1-D* individuals displayed variable phenotypes from normal morphology to typical dwarfism (Fig. S1f). We further grew the *zed1-D* plants at 18°C till the inflorescence stem elongated and then transferred them to 28°C, and observed that such a temperature shift consequentially caused developmental retardation in *zed1-D* (Fig. 1f), reconfirming that developmental retardation in *zed1-D* is temporally dependent on high temperature.

High temperature triggers the autoimmune response in *zed1-D*

In order to explore the molecular basis of growth retardation in *zed1-D*, we compared the transcriptome of *zed1-D* with WT plants after being transferred from 18 into 28°C. As expected, such a temperature shift resulted in the decreased expressions of some development-related genes in *zed1-D*, including those involved in cell wall modification, cell differentiation and stomatal development, such as *XYLOGLUCAN ENDOTRANSGLUCOSYLASE/HYDROLASE 6* (*XTH6*), *CELL WALL INVERTASE 5* (*CWINV5*), *EXPANSIN 3* (*EXP3*), *SQUAMOSA PROMOTER*

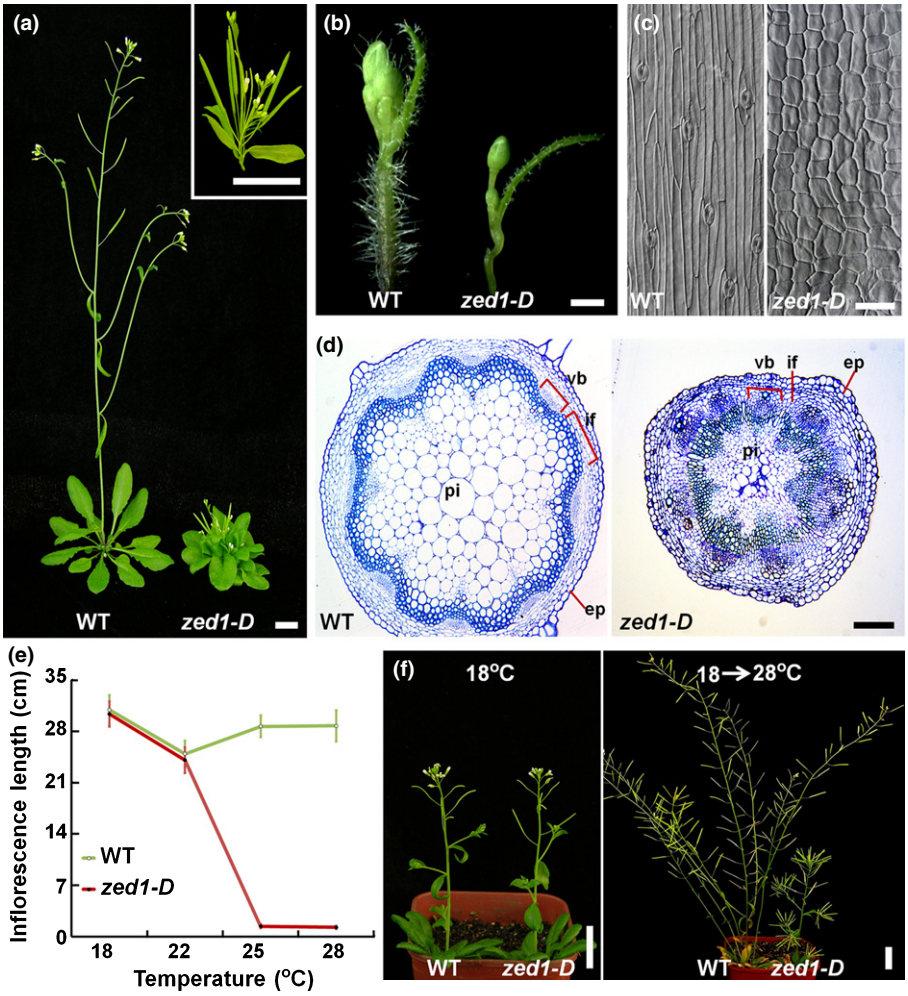

Fig. 1 High temperature-dependent growth defect in the *Arabidopsis zed1-D* mutant. (a) Morphology of 6-wk-old wild-type (WT) and *zed1-D* plants grown at 25°C. The inset shows a compressed inflorescence stem of *zed1-D*. (b) Morphology of juvenile inflorescence stems of 4-wk-old WT and *zed1-D* grown at 25°C. (c) Epidermal cells of cleared inflorescence stems of 6-wk-old WT and *zed1-D* plants grown at 25°C. (d) Cross-section of 6-wk-old inflorescence stems of WT and *zed1-D* plants grown at 25°C. vb, vascular bundle; if, interfascicular fiber; ep, epidermis; pi, pith. (e) Inflorescence stem length of 7-wk-old WT and *zed1-D* plants grown at indicated temperature conditions. Data are shown as means ± SD ($n > 10$). (f) Morphology of WT and *zed1-D* plants before and after being transferred from 18 into 28°C. WT and *zed1-D* plants were grown for 6 wk at 18°C (left panel), and then transferred to 28°C for additional 2 wk (right panel). Bars: (a) 1 cm; (b) 1 mm; (d) 100 μm; (f) 2 cm.

BINDING PROTEIN-LIKE 9 (*SPL9*) and *CYCLIN D1;1* (*CYCD1;1*) (Fig. 2a). Surprisingly, when compared with those in WT, a large number of immune-related genes were substantially upregulated in *zed1-D* (Table S3), of which 28 genes were elevated by >10 folds, including the immune marker gene *PATHOGENESIS-RELATED 1* (*PR1*), and those encoding the pathogen-inducible WRKY transcription factors, calcium-binding EF-hand family proteins, RECEPTOR-LIKE PROTEINs (RLPs), and CYSTEINE-RICH RECEPTOR-LIKE PROTEIN KINASEs (CRKs) (Fig. 2a). Further qRT-PCR analyses of a few representative genes, including *CRK23*, *WRKY46*, *EXP3* and *CWINV5*, validated that the high temperature shift indeed caused the substantial elevation of the immune-related genes but the decrease of development-related genes (Fig. 2b,c), implying that high temperature triggers the autoimmune response in *zed1-D*.

In order to verify the high temperature-dependent autoimmunity in *zed1-D*, we examined reactive oxygen species (ROS) accumulation and cell death by staining the WT and *zed1-D* plants grown at 18 or 25°C with DAB and TB, respectively. As shown in Fig. 2(d), when grown at 18°C, the *zed1-D* and WT leaves had a comparable amount of ROS production and cell death status, however, the elevated ROS content and extensive cell death were observed in the *zed1-D* plants grown at 25°C. Further expression analyses showed that the two defense marker genes, *PR1* and *PR2*, were highly elevated when *zed1-D* plants were grown at 25°C but not at 18°C (Fig. 2e), confirming the high temperature-induced autoimmune response in *zed1-D* plants.

A mutation of *ZED1* confers the pleiotropic phenotype in *zed1-D*

We then backcrossed *zed1-D* with WT plants, and observed that the F_2 progenies had a WT: *zed1-D* phenotypic segregation ratio of 3 : 1 (338 : 123, $\chi^2 = 0.60$, $P > 0.05$) when grown at

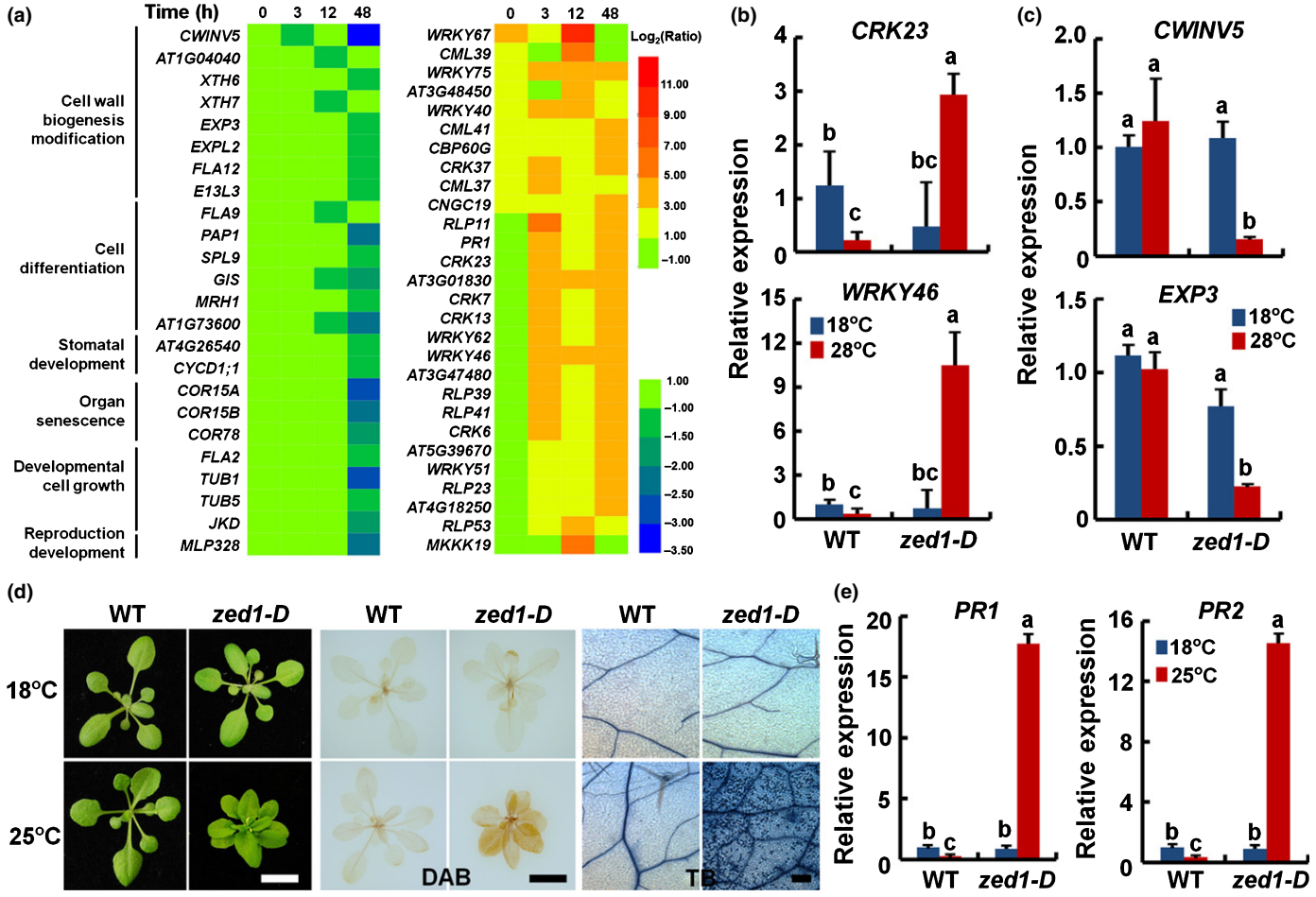

Fig. 2 High temperature triggers autoimmunity in *zed1-D*. (a) Clustering display of the differentially expressed genes between 4-wk-old *zed1-D* and wild-type (WT) after being transferred from 18 to 28°C. The expression levels of genes in *zed1-D* were calculated vs those in WT at each time point, and data are shown as an average (log_2 ratio) of two biological replicates of RNA-seq. (b, c) quantitative real-time reverse transcription PCR (qRT-PCR) analysis of the representative genes related to (b) immunity and (c) development in 4-wk-old WT and *zed1-D* plants before and after being transferred from 18 to 28°C for 48 h. (d) Diaminozenzidine (DAB) (middle panels) and Trypan Blue (TB) (right panels) stained WT and *zed1-D*. Plants were grown at 22°C for 2 wk and then transferred to 18 or 25°C for another 2 wk (left panels). Bars: (left and middle panels) 1 cm; (right panels) 100 μm. (e) Expression of the immune marker *PR1* and *PR2* genes in 4-wk-old WT and *zed1-D* plants grown at 18 or 25°C. Data are shown as means ± SD ($n = 3$), and the lowercase letters indicate the significance ($P < 0.05$) according to one-way ANOVA tests.

25°C, implying that the phenotype of *zed1-D* is caused by a mutation of a single gene. We next crossed *zed1-D* with the Landsberg accession, and finely mapped *ZED1* to an 81-kb region of the F15B8 BAC on chromosome 3 (Fig. 3a). Sequencing of the genes in this region enabled us to identify an A518G transition in At3G57750 (previously known as *HOPZ-ETI-DEFICIENT 1*, *ZED1*), leading to an N173S substitution in ZED1 (Fig. 3a). Expression analysis showed that this mutation did not affect the transcription of *ZED1* (Fig. 3b). To test whether the mutation in *ZED1* is responsible for the pleiotropic phenotype of *zed1-D*, we introduced the *p35S::ZED1* and *pZED1::ZED1* constructs into *zed1-D* plants. We found that all of the transgenic *zed1-D* plants carrying a *p35S::ZED1* construct displayed WT morphology at 25°C (Fig. 3c), demonstrating that the phenotype of *zed1-D* is caused by the mutation of *ZED1*. Interestingly, the 19 T_1 transgenic *zed1-D* plants carrying a single insertion of the *pZED1::ZED1* exhibited a semi-dwarf phenotype, and only T_2 homozygotes were fully restored into WT morphology at 25°C (Fig. 3d), suggesting that the mutation of ZED1 in the *zed1-D* has a dose effect. To verify this, we generated a *p35S::ZED1-D* (*mutated-ZED1* in *zed1-D*) construct and introduced into WT plants, and found that overexpression of *ZED1-D* caused an arrest of organ development in these transgenic seedlings (Fig. 3e,f), confirming that ZED1-D acts in a dose-dependent manner. Thus, our newly identified mutant was designated as *zed1-D* accordingly.

High temperature-induced autoimmunity in *zed1-D* is dependent on ZAR1

Recent studies have shown that *Arabidopsis* ZED1 could interact with ZAR1 to specifically meditate the effector HopZ1a-triggered immune response (Lewis *et al.*, 2013; Wang *et al.*, 2015). We thus tested whether or not the ZED1-D-tiggered autoimmunity is associated with ZAR1 by crossing *zed1-D* with *zar1-3*, a loss-of-function mutant of *ZAR1* (Lewis *et al.*, 2010). We observed that disruption of *ZAR1* completely suppressed the growth retardation observed in *zed1-D* plants grown at 25°C (Figs 4a, S2a,b). Further immune assays and expression analysis of *PR1* and *PR2* in the *zed1-D zar1-3* mutant clearly showed that the autoimmune phenotype in *zed1-D* was blocked by loss-of-function of *ZAR1* (Fig. 4b,c), indicating that high temperature-induced autoimmunity in the *zed1-D* is dependent on ZAR1.

In accordance with the recent finding that ZED1 is a pseudokinase (Lehti-Shiu & Shiu, 2012; Lewis *et al.*, 2013), we could not detect any kinase activity of ZED1 and ZED1-D by *in vitro* kinase assay (Fig. S2c). To test whether the mutation of ZED1-D alters its binding activity with ZAR1, we carefully examined the interaction of ZED1 and ZED1-D with ZAR1 in transgenic plants expressing GFP-tagged ZED1 or ZED1-D and MYC-tagged ZAR1. CoIP assay revealed that ZED1-D had a stronger binding activity with ZAR1 when compared with ZED1 (Fig. 4d), indicating that the mutation in ZED1-D enhances its

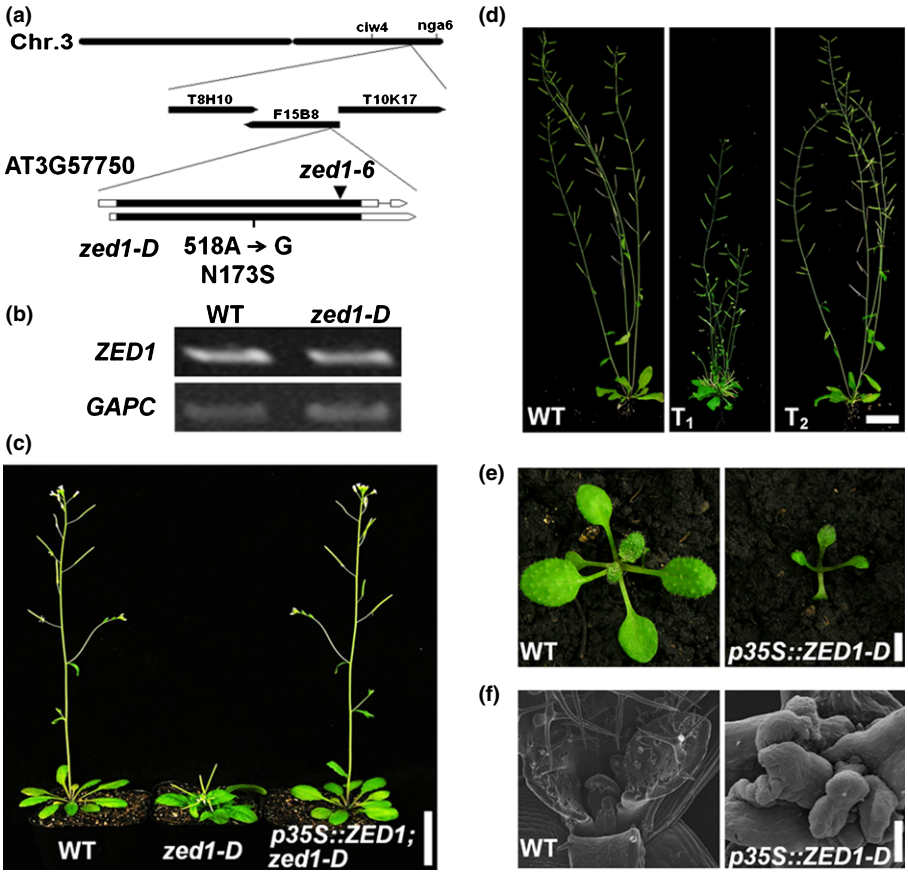

Fig. 3 Molecular cloning of *ZED1*. (a) Schematic illustration of map-based cloning and structure of *ZED1*. The molecular lesion in *zed1-D* and the T-DNA insertion site in *zed1-6* are indicated. (b) Expression of *ZED1* in 4-wk-old wild-type (WT) and *zed1-D* plants grown at 25°C. The expression of *GLYCERALDEHYDE-3-PHOSPHATE DEHYDROGENASE C SUBUNIT 1* (*GAPC*) was used as an internal control. (c) Morphology of 5-wk-old WT, *zed1-D* and *p35S::ZED1;zed1-D* plants grown at 25°C. (d) Morphology of 7-wk-old heterozygous T_1 and homozygous T_2 transgenic *zed1-D* plants harboring a *pZED1::ZED1* construct grown at 25°C. (e) Morphology and (f) the scanning electronic microscope-scanned shoot apex of 16-d-old WT and transgenic *p35S::ZED1-D* plants grown at 25°C. Bars: (c, d) 2 cm; (e) 2 mm; (f) 200 μm.

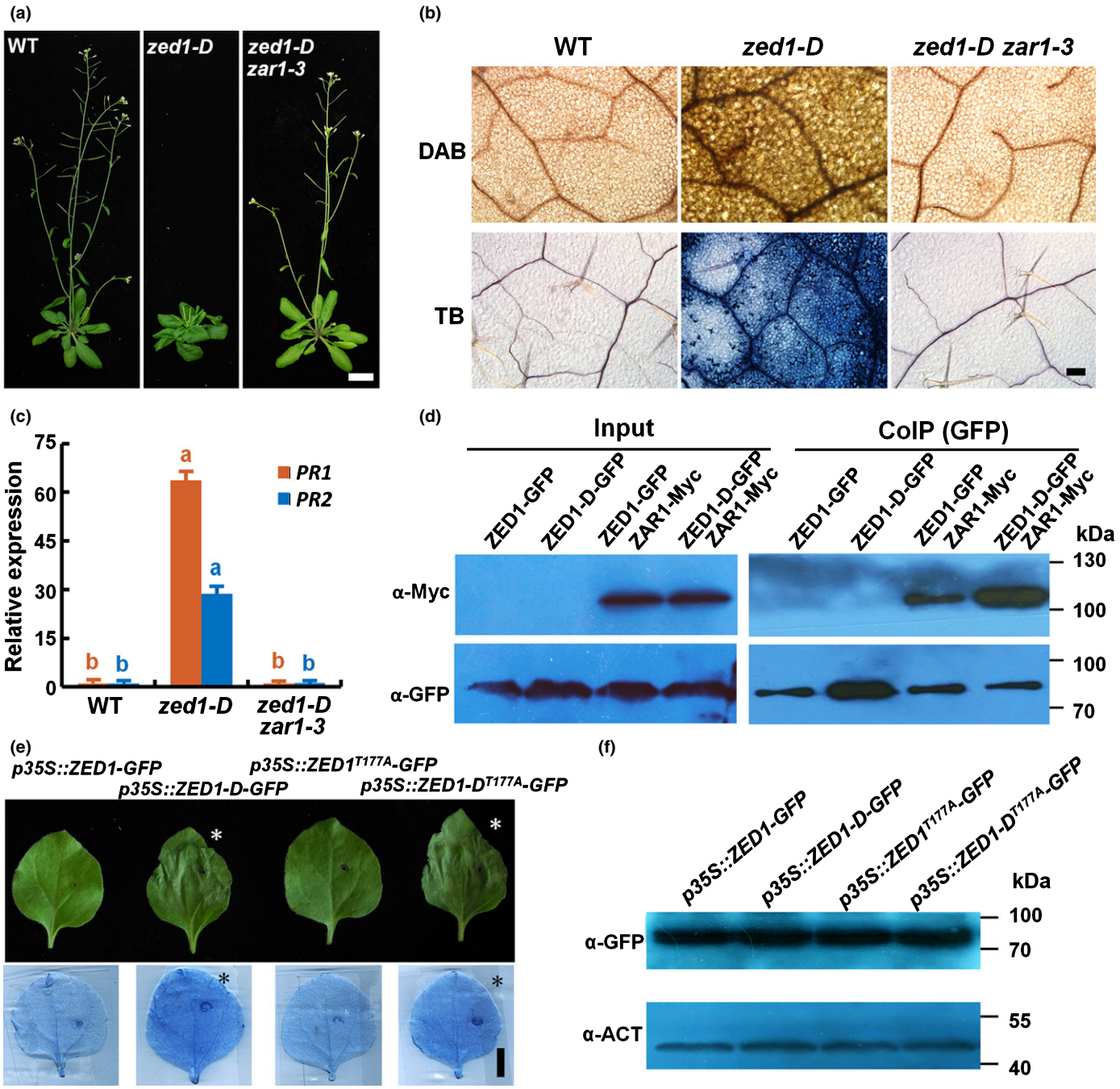

Fig. 4 *zed1-D*-triggered autoimmunity and developmental defect are *ZAR1*-dependent. (a) Phenotype of 6-wk-old wild-type (WT), *zed1-D* and *zed1-D zar1-3* plants grown at 25°C. (b) Diaminozenzidine (DAB) and Trypan Blue (TB) stained leaves of 4-wk-old WT, *zed1-D* and *zed1-D zar1-3* plants grown at 25°C. (c) *PR1* and *PR2* expression in 4-wk-old WT, *zed1-D* and *zed1-D zar1-3* plants grown at 25°C. Data are shown as means ± SD ($n = 3$). Significant differences are marked with different lowercase letters ($P < 0.05$) according to one-way ANOVA tests. (d) The enhanced interaction of ZED1-D with ZAR1. Co-immunoprecipitation (CoIP) assay was performed in 4-wk-old *Arabidopsis* transgenic plants expressing green fluorescent protein (GFP)-tagged ZED1, ZED1-D and/or Myc-tagged ZAR1 at 25°C. (e) ZED1-D-activated immune response is not dependent on acetylation of ZED1^{T177}. The leaves of 4-wk-old *Nicotiana benthamiana* plants were infiltrated with the *Agrobacterium* carrying *p35S::ZED1-GFP*, *p35S::ZED1-D-GFP*, *p35S::ZED1*^{T177A}*-GFP* or *p35S::ZED1-D*^{T177A}*-GFP* (upper panel), and then were stained with TB (lower panel) 24 h later. The hypersensitive responses (HRs) are marked with asterisks. (f) The protein accumulation of ZED1-GFP, ZED1-D-GFP, ZED1^{T177A}-GFP or ZED1-D^{T177A}-GFP in the infiltrated *N. benthamiana* leaves described in (e), and β-ACTIN (ACT) was used as an internal control. Bars, 1 cm.

interaction with ZAR1. Because the mutation of N173S in the ZED1-D is close to the T177 residue, which is acetylated by HopZ1a and largely responsible for HopZ1a-triggered ETI (Lewis *et al.*, 2013), we thus explored whether the autoimmunity activated by ZED1-D is a reminiscent acetylation of ZED1 by mutating the T177A residue of ZED1-D. As shown in

Fig. 4(e, f), the transient expression of GFP-tagged proteins in *Nicotiana benthamiana* leaves showed that the mutation of T177A in ZED1-D had no obvious effect on ZED1-D-triggered hypersensitive response (HR), suggesting that ZED1-D-triggered autoimmunity is not dependent on the acetylation of T177 in ZED1-D.

ZED1 is induced by elevated temperature and ZED1-D is exclusively localized in cytosol

In order to investigate the tissue-specific expression of *ZED1*, we generated transgenic plants harboring a *pZED1::ZED1-GUS* construct. GUS staining assay showed that *ZED1* was expressed in seedlings, juvenile rosette leaves, floral organs and inflorescence stems (Fig. S3). Further RNA *in situ* hybridization validated that the *ZED1* mRNA was accumulated in the juvenile leaves, shoot apical meristems and inflorescence stems (Fig. 5a). More importantly, both qRT-PCR and GUS staining assays revealed that *ZED1* transcripts were induced by the elevation of ambient temperature (Fig. 5b,c), implicating that ZED1 is responsive to ambient temperature. Next, we examined the subcellular localization of ZED1 and ZED1-D using transgenic plants harboring a *pZED1::ZED1-GFP* or *pZED1::ZED1-D-GFP* construct. As shown in Fig. 5(d), the ZED1-GFP signals were observed not only in cytosol, but also in the nuclei of epidermal cells in both petiole and lamina, however, the ZED1-D-GFP signals were only detectable in the cytosol, implicating that the mutation in ZED1-D prohibits it from being localized into nuclei. To verify this, we fractionated the nuclear and cytosolic proteins from these transgenic plants before and after being transferred from 18 to 25°C, and immunoblot analysis clearly showed that ZED1 was both nucleus- and cytosol-localized, whereas ZED1-D was only detectable in cytosol (Fig. 5e), confirming that the mutation in ZED1-D alters its subcellular localization. Moreover, the elevation of temperature increased the abundance of nuclear and cytosolic ZED1 or cytosolic ZED1-D but did not appear to change their cellular localizations (Fig. 5e).

ZED1 and ZRKs act cooperatively to inhibit immune response in absence of pathogen

Previous studies reveal that ZED1 and ZRK1/RKS1 are specifically required for the effector HopZ1a- and AvrAC-triggered ETI, respectively (Lewis *et al.*, 2013; Wang *et al.*, 2015).

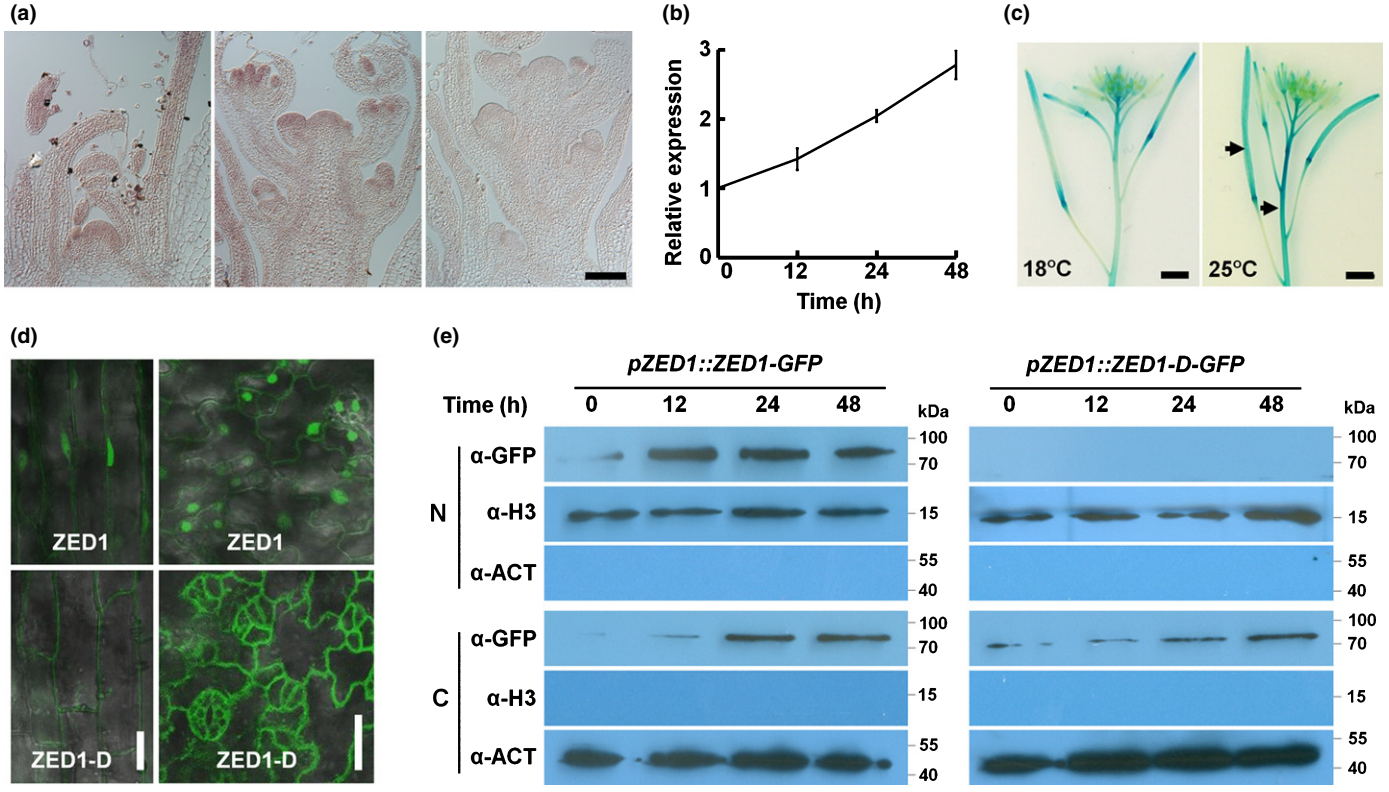

Fig. 5 Induction of ZED1 by elevated temperature and cellular localization of ZED1 and ZED1-D. (a) RNA *in situ* hybridization assayed *ZED1* transcripts in shoot apex (left) and inflorescence (middle). A hybridized sample with *ZED1* sense probe was shown in the right panel. (b) Induction of ZED1 by elevated temperature. The relative expression levels of *ZED1* were assayed with 4-wk-old wild-type (WT) plants after being transferred from 18 to 25°C for indicated times, and data are shown as means ± SD ($n = 3$). (c) The GUS staining assay on 6-wk-old transgenic *pZED1::ZED1-GUS* plants grown at 18 or 25°C. (d, e) Subcellular localization of ZED1 and ZED1-D. The green fluorescent protein (GFP) signals (d) were visualized in epidermal cells of petioles (left panel) and leaves (right panel) in 1-wk-old transgenic *pZED1::ZED1-GFP* or *pZED1::ZED1-D-GFP* plants grown at 25°C. The fractionated nuclear (N) and cytosolic (C) proteins from the above 4-wk-old transgenic plants transferred from 18 to 25°C were immunoblotted, and the Histone H3 (H3) and β-ACTIN (ACT) were used as nuclear and cytosolic internal controls, respectively (e). Bars: (a) 200 μm; (c) 2 mm; (d) 50 μm.

However, our finding that ZED1 is induced by elevated temperature and ZED1-D-triggered autoimmunity is high temperature-dependent implies that ZED1 or ZRKs also might be involved in the regulation of the ambient temperature-sensitive intersection of growth and immune response in the absence of pathogens. Because the RLCK XII-2 gene subfamily contains 13 *ZRK*s clustered on chromosome 1 and 3 with the differential and overlapped expression patterns (Fig. S4a–c), we first tested the possible functional redundancy of ZRKs by overexpressing each of them in *zed1-D* plants. We observed that overexpression of *ZRK1* or *ZRK12* could fully rescue the *zed1-D* phenotype and overexpression of *ZRK4*, *ZRK10*, *ZRK13* or *ZRK14* could partially do so (Fig. 6a). Moreover, expression analyses showed that the transcriptions of *ZRK1*, *ZRK6* and *ZRK12* but not *ZRK4* were induced by elevated temperature (Fig. 6b). These observations suggest that some ZRKs function redundantly with ZED1 in ambient temperature-sensitive immune response in absence of pathogen. To verify this, we obtained the T-DNA insertion mutant of *ZED1*, *zed1-6*, which is specifically defective in HopZ1a-triggered ETI (Lewis *et al.*, 2013). However, we could not observe any developmental defect in the *zed1-6* plants when grown at 25°C (Figs 6c, S4d). We next obtained a T-DNA insertion mutant of *ZRK12*, *zrk12-1* and further generated the *zed1-6 zrk12-1* double mutant. The *zrk12-1* plants displayed a slightly shortened inflorescence stem, and such a phenotype was found to be enhanced in the *zed1-6 zrk12-1* double mutant when grown at 25°C (Figs 6c, S4d). Immune assays and expression analysis of *PR1* and *PR2* revealed that *zed1-6 zrk12-1* plants grown at 25°C but not at 18°C had a lesion characteristic of autoimmunity (Fig. 6d,e), supporting that ZED1 and ZRKs function redundantly and cooperatively to inhibit the immunity in response to elevation of ambient temperature.

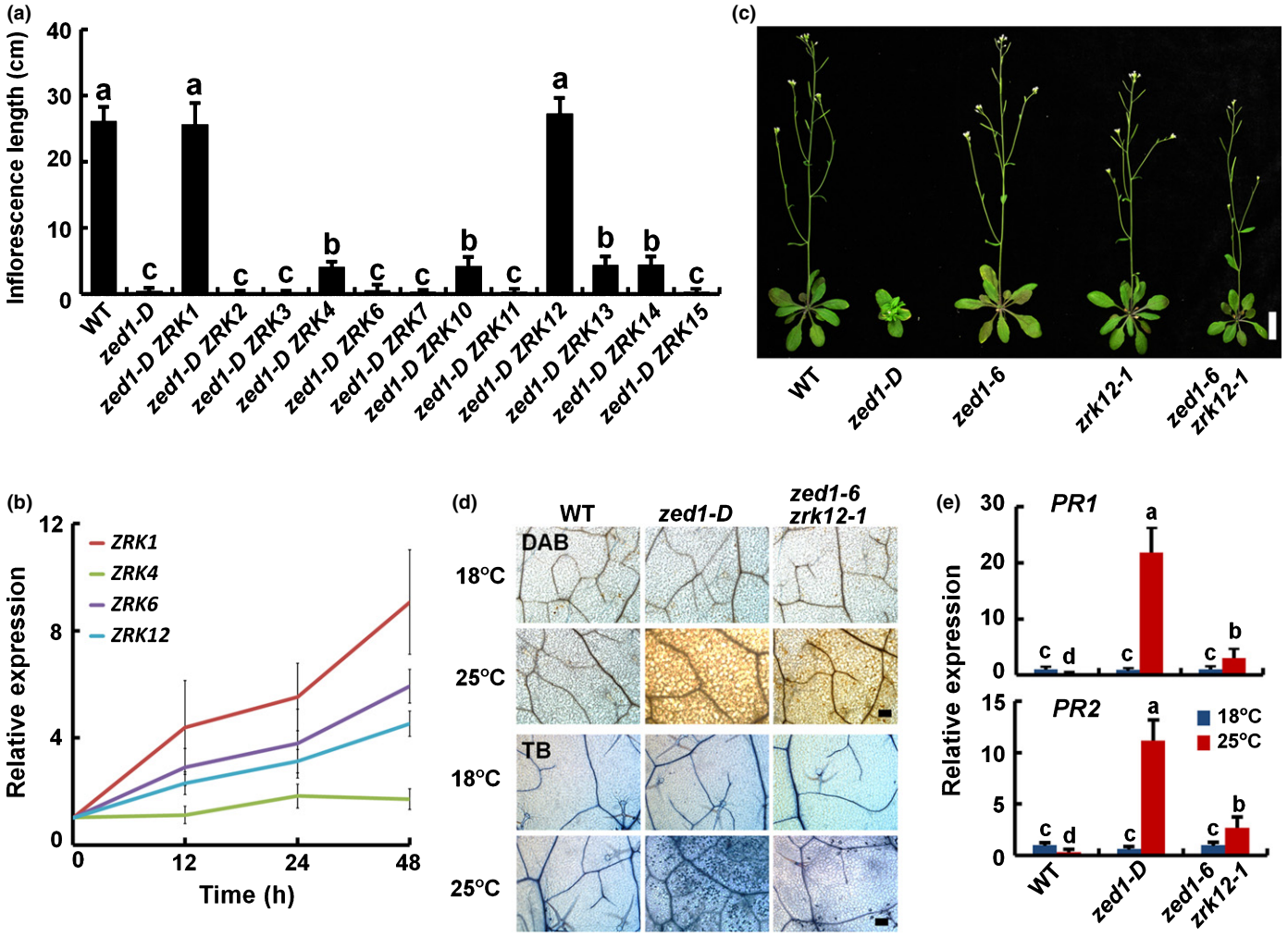

Fig. 6 ZED1-related kinases (ZRKs) act cooperatively in mediating temperature-sensitive immune response and development. (a) Complementation of *zed1-D* by overexpressed *ZRK*s. The inflorescence stem length of 6-wk-old transgenic *zed1-D* plants carrying each *p35S::ZRK* construct at 25°C was measured. (b) Expression of *ZRK1*, *ZRK4*, *ZRK6* and *ZRK12* in 4-wk-old wild-type (WT) plants after being transferred from 18 to 25°C for indicated times, and the data are shown as means ± SD ($n = 3$). (c) Morphology of 6-wk-old WT, *zed1-D*, *zed1-6*, *zrk12-1* and *zed1-6 zrk12-1* plants grown at 25°C. (d) Diaminozenzidine (DAB) and Trypan Blue (TB) staining of 4-wk-old WT, *zed1-D* and *zed1-6 zrk12-1* plants grown at 18 or 25°C. (e) Expression of *PR1* and *PR2* in 4-wk-old WT, *zed1-D* and *zed1-6 zrk12-1* plants grown at 18 or 25°C. Data are shown as means ± SD ($n = 3$), and the lowercase letters indicate the significance ($P < 0.05$) according to one-way ANOVA tests. Bars: (c) 2 cm; (d) 100 μm.

ZED1 meditates the immune response by modulating *SNC1* transcription

Previous studies have suggested that the *Arabidopsis* SNC1 is a downstream regulator of temperature-sensitive autoimmunity (Gou & Hua, 2012). We thus speculated whether ZED1-mediated immunity is dependent on or through the regulation of *SNC1*. To test this, we first monitored the expression of *SNC1* in the *zed1-D*, and found that the transcription of *SNC1* was indeed elevated when *zed1-D* plants were grown at 25 but not 18°C (Fig. 7a). Consistently, the expression of *SNC1* was also found to be increased in the *zed1-6 zrk12-1* at 25°C (Fig. 7a), suggesting that ZED1 and some ZRKs play an inhibitory role in regulating *SNC1* transcription. To verify this, we further overexpressed *ZED1* in the gain-of-function mutant of *SNC1*, *ball/snc1-2*, and observed that overexpression of *ZED1* could rescue the developmental defect and suppress the overexpressed *SNC1* in *ball/snc1-2* at 22°C (Fig. 7b,c). Consequently, the autoimmune phenotype of *ball/snc1-2*, including the activated *PR1* and *PR2*, elevated ROS and enhanced cell death, was fully suppressed by overexpression of *ZED1* (Fig. 7d,e). This finding indicates that the inhibitory role of ZED1 and ZRKs in the regulation of immune responses is, at least in part, through suppressing the *SNC1* transcription.

In order to further verify that SNC1 acts downstream of ZED1-mediated basal immunity, we next crossed *zed1-D* with the loss-of-function mutant of *SNC1*, *snc1-11*, and generated the double mutant *zed1-D snc1-11*. As expected, disruption of *SNC1* fully restored the developmental defect and blocked the autoimmunity of *zed1-D* at 25°C (Fig. 7f–h). In addition, it has been reported that SNC1-triggered immunity is dependent on salicylic acid (SA) production (Yang & Hua, 2004), we thus crossed the *zed1-D* with the transgenic plants overexpressing the *naphthalene hydroxylase G* (*nahG*), which encodes an enzyme catalyzing SA degradation (Bowling *et al.*, 1994). Our results showed that overexpression of *nahG* could rescue the autoimmune and developmental defects of *zed1-D* at 25°C (Fig. S5). Taken together, we conclude that SNC1 acts downstream of ZED1 or ZRKs to mediate the temperature-sensitive immune response in the absence of pathogens.

Discussion

Ambient temperature is a major environmental factor that regulates many aspects of plant growth and development, including seed germination, plant growth, flowering, hormonal responses and immune response (Penfield, 2008; Hua, 2013). In *Arabidopsis*, a large number of autoimmune mutants with retarded development have been identified and shown to be dependent on low temperature, indicating that ambient temperature plays an important role in balancing the basal immune response and growth homeostasis in the absence of pathogens (Huot *et al.*, 2014). Recent works in *Arabidopsis* have suggested that the decreased accumulation of nuclear resistance (R) proteins, including SNC1, is a possible regulatory mechanism for the dampened ETI response under high temperature conditions (Elmore *et al.*, 2011; Heidrich *et al.*, 2012; Hua, 2013); however, the molecules that link ambient temperature and immune response remain elusive. Here, we identified and characterized an *Arabidopsis* autoimmune mutant *zed1-D*. Surprisingly, we found that, unlike other previously identified autoimmune mutants that are sensitive to low temperature, *zed1-D* exhibits a high temperature-dependent autoimmune phenotype. To our knowledge, *zed1-D* is the first reported high temperature-sensitive autoimmune mutant so far. Our further work demonstrates that ZED1 and some ZED1-related kinases (ZRKs) are induced by the high temperature, and that ZRKs act redundantly and cooperatively to inhibit the immune response by suppressing *SNC1* transcription in the absence of pathogens. Although the molecular regulation of ZRKs by ambient temperature and of *SNC1* by ZRK remain to be further clarified, our results define the ZRKs as a molecular link of ambient temperature cue and immune response in the absence of pathogens, and thus outline a possible molecular pathway of the ambient temperature-regulated intersection of immune response and growth in plants (Fig. 8).

Arabidopsis ZRKs have been defined as cytoplasmic RLKs, and ZED1 and ZRK1/RKS1 are shown to be specifically required for the effector HopZ1a- and AvrAC-triggered ETI response via interaction with HOPZ-ACTIVATED RESISTANCE 1 (ZAR1), respectively (Lewis *et al.*, 2013; Wang *et al.*, 2015). However, we show here that a dominant mutation of ZED1 results in a high temperature-dependent autoimmunity in absence of pathogens. ZED1 and some ZRK members are responsive to high temperature, and the loss of function of both *ZED1* and *ZRK12* leads to a high temperature-dependent lesion of autoimmunity, whereas overexpression of *ZED1* could suppress the SNC1-activated autoimmunity. Because multiple *ZRK* genes are responsive to ambient temperature and some ZRKs function redundantly, it is expected that *zed1-6 zed12-1* plants display a weak autoimmune phenotype when compared with *zed1-D*. Therefore, it is likely that, besides their specific roles in activation of the effector-triggered ETI in presence of pathogens, ZRKs also function cooperatively to balance the immunity and development in response to ambient temperature or possible other environmental cues by fine-tuning the *SNC1* transcription in the absence of pathogens. However, because the two identified ZRK members, ZED1 and ZRK1, could interact with ZAR1, and ZED1-D triggered autoimmunity is dependent on ZAR1, it remains unclear whether the inhibitory role of ZRK-ZAR1 complexes on *SNC1* in the absence of pathogens is through the downstream events or by antagonizing the interaction of ZRKs with other factors. In addition, ZED1 is nucleus- and cytosol-localized, whereas ZED1-D is exclusively localized in cytosol, and it is also of interest whether the nuclear ZRKs contribute to the inhibition of the immune response in the absence of pathogens.

Recently, some *Arabidopsis* autoimmune mutants, including *bon1*, *bap1*, *bir1*, *mkp1* and *cpr1*, were found to be low temperature-sensitive and SNC1-dependent, because their autoimmune phenotype is observed at or below 22°C but is partially or fully abolished when plants are grown at 28°C or by loss-of-function of *SNC1* (Yang & Hua, 2004; Yang *et al.*, 2006; Bartels *et al.*,

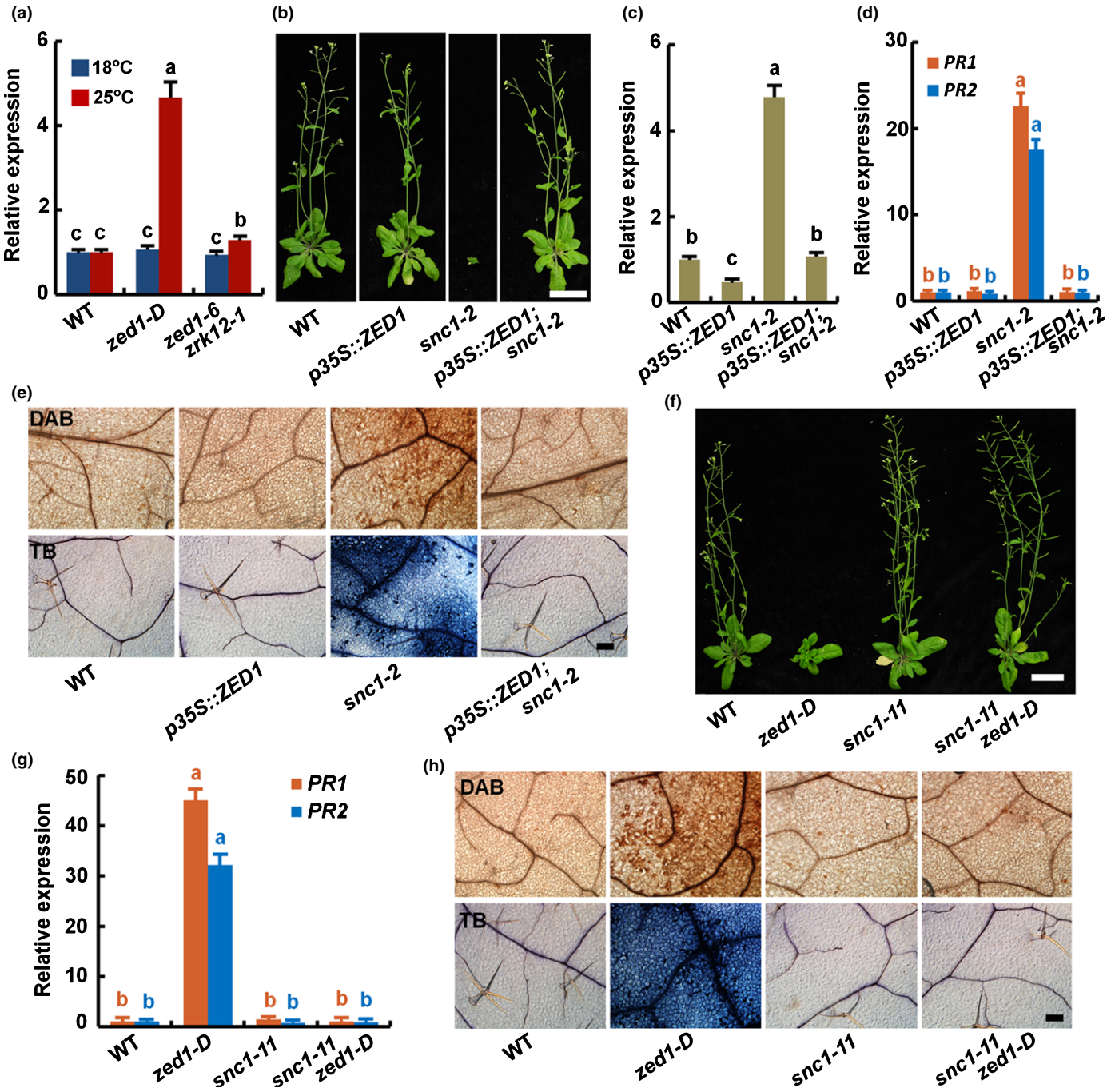

Fig. 7 SNC1 acts downstream of ZED1-mediated immunity. (a) Expression of *SNC1* in 4-wk-old wild-type (WT), *zed1-D* and *zed1-6 zrk12-1* plants grown at 18 or 25°C. Data are shown as means ± SD ($n = 3$), and the lowercase letters indicate the significance ($P < 0.05$) according to one-way ANOVA tests. (b) Morphology of 6-wk-old WT, *p35S:ZED1*, *snc1-2* and *p35S:ZED1;snc1-2* plants grown at 22°C. (c) Expression of *SNC1* in 4-wk-old WT, *p35S:ZED1*, *snc1-2* and *p35S:ZED1;snc1-2* plants grown at 22°C. Data are shown as means ± SD ($n = 3$), and the lowercase letters indicate the significance ($P < 0.05$) according to one-way ANOVA tests. (d) Expression analysis of *PR1* and *PR2* in 4-wk-old WT, *p35S:ZED1*, *snc1-2* and *p35S:ZED1;snc1-2* plants grown at 22°C, and different lower case letters indicate significance ($P < 0.05$) according to one-way ANOVA tests. (e) Diaminozenzidine (DAB) and Trypan Blue (TB) stained leaves of 4-wk-old WT, *p35S:ZED1*, *snc1-2* and *p35S:ZED1;snc1-2* plants grown at 22°C. (f) Morphology of 6-wk-old WT, *zed1-D*, *snc1-11* and *snc1-11 zed1-D* plants grown at 25°C. (g) Expression of *PR1* and *PR2* in 4-wk-old WT, *zed1-D*, *snc1-11* and *snc1-11 zed1-D* plants grown at 25°C. Data are shown as means ± SD ($n = 3$), and the lowercase letters indicate the significance ($P < 0.05$) according to one-way ANOVA tests. (h) DAB and TB stained leaves of 4-wk-old WT, *zed1-D*, *snc1-11* and *snc1-11 zed1-D* plants grown at 25°C. Bars: (b, f) 2 cm; (e, h) 100 μm.

2009; Cheng *et al.*, 2011; Wang *et al.*, 2011b; Gou & Hua, 2012). Moreover, high ambient temperatures could reduce the nuclear accumulation of SNC1, which contributes to the repression of defense responses at elevated temperature (Zhu *et al.*, 2010). These pieces of evidence strongly suggest that, besides its critical role in the pathogen-induced immune

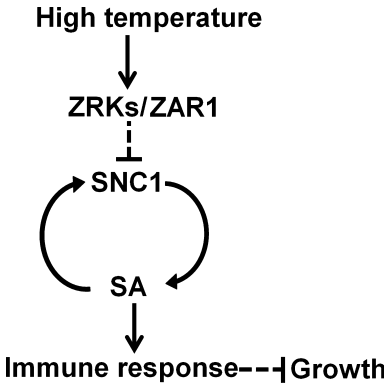

Fig. 8 A proposed model for ZED1-related kinase (ZRK)-regulated intersection of immune response and growth. SA, salicylic acid.

response, SNC1 also play an important role in mediating the temperature-sensitive intersection of plant immune response in the absence of pathogens. Here, we demonstrate that the high temperature-dependent autoimmune phenotype in *zed1-D* is due to the elevated expression of *SNC1*, and that loss-of-function of *ZED1* and *ZRK12* causes a high temperature-dependent de-repression of *SNC1*. Moreover, we show that overexpression of *ZED1* suppresses this SNC1-triggered autoimmunity by inhibiting *SNC1* transcription. These observations demonstrate that SNC1 is also a downstream player of the ZRK-mediated intersection of immune response and growth under normal growth conditions. Therefore, our results, together with those in previous works, strongly suggest that the fine-tuning of SNC1 might be a regulatory mechanism behind the regulation of immunity by ambient temperature or possible other environmental cues in plants. Recent studies reveal that SNC1 is regulated at both transcriptional and post-transcriptional levels by multiple regulatory networks (Johnson *et al.*, 2012). For example, genetic screens have identified multiple members of the MODIFIER OF *snc1* (MOS) and MUTANT *snc1*-ENHANCING (MUSE) (Johnson *et al.*, 2012, 2015), among which MOS1 and MOS9 upregulate the transcription of *SNC1* through chromatin remodeling, whereas MOS2, MOS4 and MOS12 are required for proper splicing of the transcripts of *SNC1*, and MUSE13 and MUSE14 contribute to the turnover of SNC1 (Johnson *et al.*, 2012, 2015; Huang *et al.*, 2016). Therefore, it remains to be clarified whether the inhibition of *SNC1* transcription by ZRK–ZAR1 complexes is through these regulators and/or dependent on other unidentified components. We could not exclude the possible post-transcriptional regulation of this process, either. In addition, because the decreased accumulation of nuclear SNC1 is a possible regulatory mechanism for a dampened immune response under high temperature conditions (Zhu *et al.*, 2010; Mang *et al.*, 2012), it is also of interest to carefully examine whether the high temperature has any effect on subcellular distribution of ZRKs in the absence of pathogens.

Because ZRKs and SNC1 are involved in both low and high temperature-sensitive autoimmunity, it is likely that the transcriptional suppression of *SNC1* by ZRKs represents a previously unidentified regulatory mechanism underlying the ambient temperature-mediated immune response. Under low ambient temperature conditions, the comparatively low content of ZED1 or ZRKs is likely sufficient to maintain plant immunity by fine-tuned *SNC1* expression in the absence of pathogens. When ambient temperature elevates, the high temperature-induced ZRKs or ZRK–ZAR1 complexes are required to dampen the immune response and allow plant growth. By contrast, a low content of cytosolic ZED1-D in *zed1-D* may not be sufficient to cause the autoimmune phenotype under low temperature conditions, whereas the highly cytosolic accumulation of ZED1-D induced by elevated temperature results in the over-activation of *SNC1*, thus conferring *zed1-D* plants with autoimmune responses and developmental defects. Notably, as the *zed1-D* growth defect can be completely restored by disruption of *SNC1* or removal of salicylic acid, it also is likely that the growth retardation of *zed1-D* is a result of immune activation. Thus, the ZRKs may function mainly in regulating the immune response, which in turn antagonizes growth and development in a temperature-sensitive manner. Because *zed1-D* is the first identified high temperature-sensitive autoimmune mutant and ZRKs function in the absence and presence of pathogens, further characterization of the *zed1-D*- and ZRK-mediated immune response in both cases will shed more light on ambient temperature-mediated immune responses and their intersection with growth homeostasis in plants.

Acknowledgements

We are grateful to S. H. Yang, N. H. Chua and R. C. Lin for kindly providing the bacterial strains, vectors and mutant seeds used in this study. We also are grateful to ABRC for the mutant lines. We thank F. Q. Dong for technical assistance in semi-thin section preparation. This work was supported by the National Natural Science Foundation of China (31471160 and 31121065).

Author contributions

Y.H. conceived the project; Y.H., D.C., D.R. and D.T. designed the experiments; Z.W., J.L. and D.C. performed most of the experiments; C.L., J.Z., Y.L. and N.L. worked on the transgenic lines and performed the immune and kinase assays; W.X. performed RNA *in situ* hybridization; and Y.H., D.C. and Z.W. analyzed data and wrote the paper.

References

Alcazar R, Garcia AV, Parker JE, Reymond M. 2009. Incremental steps toward incompatibility revealed by *Arabidopsis* epistatic interactions modulating salicylic acid pathway activation. *Proceedings of the National Academy of Sciences, USA* **106**: 334–339.

Bartels S, Anderson JC, Gonzalez Besteiro MA, Carreri A, Hirt H, Buchala A, Metraux JP, Peck SC, Ulm R. 2009. MAP KINASE PHOSPHATASE1 and PROTEIN TYROSINE PHOSPHATASE1 are repressors of salicylic acid synthesis and SNC1-mediated responses in *Arabidopsis*. *Plant Cell* **21**: 2884–2897.

Bomblies K, Lempe J, Epple P, Warthmann N, Lanz C, Dangl JL, Weigel D. 2007. Autoimmune response as a mechanism for a Dobzhansky–Muller-type incompatibility syndrome in plants. *PLoS Biology* **5**: e236.

Bowling SA, Guo A, Cao H, Gordon AS, Klessig DF, Dong X. 1994. A mutation in *Arabidopsis* that leads to constitutive expression of systemic acquired resistance. *Plant Cell* **6**: 1845–1857.

Cheng YT, Li Y, Huang S, Huang Y, Dong X, Zhang Y, Li X. 2011. Stability of plant immune-receptor resistance proteins is controlled by SKP1-CULLIN1-F-box (SCF)-mediated protein degradation. *Proceedings of the National Academy of Sciences, USA* **108**: 14 694–14 699.

Clarke JD. 2009. Phenotypic analysis of *Arabidopsis* mutants: diaminobenzidine stain for hydrogen peroxide. *Cold Spring Harbor Protocols* **2009**: Pdb prot4981.

Cui D, Zhao J, Jing Y, Fan M, Liu J, Wang Z, Xin W, Hu Y. 2013. The *Arabidopsis* IDD14, IDD15, and IDD16 cooperatively regulate lateral organ morphogenesis and gravitropism by promoting auxin biosynthesis and transport. *PLoS Genetics* **9**: e1003759.

Elmore JM, Lin ZJ, Coaker G. 2011. Plant NB-LRR signaling: upstreams and downstreams. *Current Opinion in Plant Biology* **14**: 365–371.

Fobert PR, Coen ES, Murphy GJ, Doonan JH. 1994. Patterns of cell division revealed by transcriptional regulation of genes during the cell cycle in plants. *EMBO Journal* **13**: 616–624.

Gomez-Gomez L, Felix G, Boller T. 1999. A single locus determines sensitivity to bacterial flagellin in *Arabidopsis thaliana*. *Plant Journal* **18**: 277–284.

Gou M, Hua J. 2012. Complex regulation of an *R* gene *SNC1* revealed by auto-immune mutants. *Plant Signaling & Behavior* **7**: 213–216.

Heidrich K, Blanvillain-Baufume S, Parker JE. 2012. Molecular and spatial constraints on NB-LRR receptor signaling. *Current Opinion in Plant Biology* **15**: 385–391.

Hu Y, Bao F, Li J. 2000. Promotive effect of brassinosteroids on cell division involves a distinct CycD3-induction pathway in *Arabidopsis*. *Plant Journal* **24**: 693–701.

Hu Y, Xie Q, Chua NH. 2003. The *Arabidopsis* auxin-inducible gene *ARGOS* controls lateral organ size. *Plant Cell* **15**: 1951–1961.

Hu Z, Qin Z, Wang M, Xu C, Feng G, Liu J, Meng Z, Hu Y. 2010. The *Arabidopsis* SMO2, a homologue of yeast TRM112, modulates progression of cell division during organ growth. *Plant Journal* **61**: 600–610.

Hua J. 2013. Modulation of plant immunity by light, circadian rhythm, and temperature. *Current Opinion in Plant Biology* **16**: 406–413.

Huang S, Chen X, Zhong X, Li M, Ao K, Huang J, Li X. 2016. Plant TRAF proteins regulate NLR immune receptor turnover. *Cell Host & Microbe* **19**: 204–215.

Huang X, Li J, Bao F, Zhang X, Yang S. 2010. A gain-of-function mutation in the *Arabidopsis* disease resistance gene *RPP4* confers sensitivity to low temperature. *Plant Physiology* **154**: 796–809.

Huot B, Yao J, Montgomery BL, He SY. 2014. Growth-defense tradeoffs in plants: a balancing act to optimize fitness. *Molecular Plant* **7**: 1267–1287.

Jing Y, Cui D, Bao F, Hu Z, Qin Z, Hu Y. 2009. Tryptophan deficiency affects organ growth by retarding cell expansion in *Arabidopsis*. *Plant Journal* **57**: 511–521.

Johnson KC, Dong OX, Huang Y, Li X. 2012. A rolling stone gathers no moss, but resistant plants must gather their moses. *Cold Spring Harbor Symposia on Quantitative Biology* **77**: 259–268.

Johnson KC, Xia S, Feng X, Li X. 2015. The chromatin remodeler SPLAYED negatively regulates SNC1-mediated immunity. *Plant Cell Physiology* **56**: 1616–1623.

Jones JD, Dangl JL. 2006. The plant immune system. *Nature* **444**: 323–329.

Lehti-Shiu MD, Shiu SH. 2012. Diversity, classification and function of the plant protein kinase superfamily. *Philosophical Transactions of the Royal Society B: Biological Sciences* **367**: 2619–2639.

Lewis JD, Lee AH, Hassan JA, Wan J, Hurley B, Jhingree JR, Wang PW, Lo T, Youn JY, Guttman DS *et al.* 2013. The *Arabidopsis* ZED1 pseudokinase is required for ZAR1-mediated immunity induced by the *Pseudomonas syringae* type III effector HopZ1a. *Proceedings of the National Academy of Sciences, USA* **110**: 18722–18727.

Lewis JD, Wu R, Guttman DS, Desveaux D. 2010. Allele-specific virulence attenuation of the *Pseudomonas syringae* HopZ1a type III effector via the *Arabidopsis* ZAR1 resistance protein. *PLoS Genetics* **6**: e1000894.

Liu L, Zhang Y, Tang S, Zhao Q, Zhang Z, Zhang H, Dong L, Guo H, Xie Q. 2010. An efficient system to detect protein ubiquitination by agroinfiltration in *Nicotiana benthamiana*. *Plant Journal* **61**: 893–903.

Mang HG, Qian W, Zhu Y, Qian J, Kang HG, Klessig DF, Hua J. 2012. Abscisic acid deficiency antagonizes high-temperature inhibition of disease resistance through enhancing nuclear accumulation of resistance proteins SNC1 and RPS4 in *Arabidopsis*. *Plant Cell* **24**: 1271–1284.

McDowell JM, Simon SA. 2006. Recent insights into *R* gene evolution. *Molecular Plant Pathology* **7**: 437–448.

Mittler R, Shulaev V, Lam E. 1995. Coordinated activation of programmed cell death and defense mechanisms in transgenic tobacco plants expressing a bacterial proton pump. *Plant Cell* **7**: 29–42.

Molina A, Volrath S, Guyer D, Maleck K, Ryals J, Ward E. 1999. Inhibition of protoporphyrinogen oxidase expression in *Arabidopsis* causes a lesion-mimic phenotype that induces systemic acquired resistance. *Plant Journal* **17**: 667–678.

Penfield S. 2008. Temperature perception and signal transduction in plants. *New Phytologist* **179**: 615–628.

Roux M, Schwessinger B, Albrecht C, Chinchilla D, Jones A, Holton N, Malinovsky FG, Tor M, de Vries S, Zipfel C. 2011. The *Arabidopsis* leucine-rich repeat receptor-like kinases BAK1/SERK3 and BKK1/SERK4 are required for innate immunity to hemibiotrophic and biotrophic pathogens. *Plant Cell* **23**: 2440–2455.

Stokes TL, Kunkel BN, Richards EJ. 2002. Epigenetic variation in *Arabidopsis* disease resistance. *Genes & Development* **16**: 171–182.

Wang Z, Meng P, Zhang X, Ren D, Yang S. 2011b. BON1 interacts with the protein kinases BIR1 and BAK1 in modulation of temperature-dependent plant growth and cell death in *Arabidopsis*. *Plant Journal* **67**: 1081–1093.

Wang G, Roux B, Feng F, Guy E, Li L, Li N, Zhang X, Lautier M, Jardinaud MF, Chabannes M *et al.* 2015. The decoy substrate of a pathogen effector and a pseudokinase specify pathogen-induced modified-self recognition and immunity in plants. *Cell Host & Microbe* **18**: 285–295.

Wang W, Ye R, Xin Y, Fang X, Li C, Shi H, Zhou X, Qi Y. 2011a. An importin beta protein negatively regulates MicroRNA activity in *Arabidopsis*. *Plant Cell* **23**: 3565–3576.

van Wees S. 2008. Phenotypic analysis of *Arabidopsis* mutants: Trypan blue stain for fungi, oomycetes, and dead plant cells. *Cold Spring Harbor Protocols* **2008**: Pdb prot4982.

Xu J, Li Y, Wang Y, Liu H, Lei L, Yang H, Liu G, Ren D. 2008. Activation of MAPK kinase 9 induces ethylene and camalexin biosynthesis and enhances sensitivity to salt stress in *Arabidopsis*. *Journal of Biological Chemistry* **283**: 26 996–27 006.

Yang S, Hua J. 2004. A haplotype-specific *Resistance* gene regulated by *BONZAI1* mediates temperature-dependent growth control in *Arabidopsis*. *Plant Cell* **16**: 1060–1071.

Yang H, Li Y, Hua J. 2006. The C2 domain protein BAP1 negatively regulates defense responses in *Arabidopsis*. *Plant Journal* **48**: 238–248.

Yang H, Shi Y, Liu J, Guo L, Zhang X, Yang S. 2010. A mutant CHS3 protein with TIR-NB-LRR-LIM domains modulates growth, cell death and freezing tolerance in a temperature-dependent manner in *Arabidopsis*. *Plant Journal* **63**: 283–296.

Zhang Y, Goritschnig S, Dong X, Li X. 2003. A gain-of-function mutation in a plant disease resistance gene leads to constitutive activation of downstream signal transduction pathways in *suppressor of npr1-1, constitutive 1*. *Plant Cell* **15**: 2636–2646.

Zhou F, Mosher S, Tian M, Sassi G, Parker J, Klessig DF. 2008. The *Arabidopsis* gain-of-function mutant *ssi4* requires *RAR1* and *SGT1b* differentially for defense activation and morphological alterations. *Molecular Plant–Microbe Interactions* **21**: 40–49.

Zhu Y, Qian W, Hua J. 2010. Temperature modulates plant defense responses through NB-LRR proteins. *PLoS Pathogens* **6**: e1000844.

Supporting Information

Additional Supporting Information may be found online in the Supporting Information tab for this article:

Fig. S1 Phenotypic characterization of *zed1-D* plants.

Fig. S2 Genetic interaction of ZED1 and ZAR1.

Fig. S3 Tissue-specific expression of *ZED1* assayed in transgenic *pZED1::ZED1-GUS* plants.

Fig. S4 Phylogenetic and expression analysis of *ZRK* gene family.

Fig. S5 Genetic interaction of ZED1- and SA-dependent immunity.

Table S1 Primers used in this study

Table S2 Morphology of *zed1-D* plants

Table S3 High temperature-induced immune genes in *zed1-D*

Please note: Wiley Blackwell are not responsible for the content or functionality of any Supporting Information supplied by the authors. Any queries (other than missing material) should be directed to the *New Phytologist* Central Office.